

Influence of the Rashba effect on the Josephson current through a superconductor/Luttinger liquid/superconductor tunnel junction

I. V. Krive,^{1,2} A. M. Kadigrobov,^{1,3} R. I. Shekhter,¹ and M. Jonson¹¹*Department of Physics, Göteborg University, SE-412 96 Göteborg, Sweden*²*B. I. Verkin Institute for Low Temperature Physics and Engineering, 47 Lenin Avenue, 61103 Kharkov, Ukraine*³*Theoretische Physik III, Ruhr-Universität Bochum, D-44780 Bochum, Germany*

(Received 30 June 2004; revised manuscript received 17 January 2005; published 17 June 2005)

The Josephson current through a one-dimensional quantum wire with Rashba spin-orbit and electron-electron interactions is calculated. We show that the interplay of Rashba and Zeeman interactions gives rise to an anomalous phase shift in the current-phase relation for the supercurrent. The electron dispersion asymmetry induced by the Rashba interaction in a Luttinger-liquid wire plays a significant role when the electron-electron interaction is not strong and for poorly transmitting junctions. It is shown that for a weak or moderate electron-electron interaction the spectrum of plasmonic modes confined to the normal part of the junction becomes quasi-random in the presence of dispersion asymmetry. The resonance effects which are significant for transport properties of weakly interacting electrons in symmetric junctions survive in the presence of a strong Rashba interaction only for special boundary conditions at normal metal/superconductor interfaces.

DOI: 10.1103/PhysRevB.71.214516

PACS number(s): 71.10.Pm, 31.30.Gs, 71.70.Ej, 72.15.Nj

I. INTRODUCTION

In recent years the concept of a Luttinger liquid (LL) as a realistic model of interacting electrons in one-dimensional (1D) metallic structures has received experimental support (see, e.g., Refs. 1–5). Quantum wires (QWs) in laterally constrained 2D electron gases (2DEG) and single wall carbon nanotubes (SWNTs) are the two best known structures where LL behavior has been established both theoretically and experimentally.

In SWNTs, where the interaction effects have been shown to be strong,^{3–5} interaction can strongly influence the charge and spin transport through the nanotube. When a repulsively interacting LL is coupled to metallic leads (M) of noninteracting electrons, two qualitatively different regimes of charge transport may be realized depending on the quality of the LL/ M electrical contacts. For tunnel contacts charge transport through the system is strongly suppressed at low temperatures and low bias voltages⁶ by the repulsive electron-electron (e - e) interaction. In contrast, for adiabatic contacts when electron backscattering is negligibly small, the conductance is not renormalized by the interaction.^{7–9}

These two types of charge transport behavior also characterize the superconducting properties of a LL wire coupled to superconductors. For adiabatic contacts only Andreev scattering of electrons occurs at the boundaries between the LL and the bulk superconductors (LL/ S boundaries). This process does not lead to a redistribution of charge density along the wire and therefore the Coulomb interaction does not influence the supercurrent through a perfect LL. The above statement was proved in Ref. 10 by a direct calculation of the Josephson current through a long S /LL/ S junction $L \gg \xi_0$ (L is the junction length, $\xi_0 = \hbar v_F / |\Delta|$ is the superconducting coherence length, Δ is the superconducting order parameter). In the opposite case of a tunnel S /I/LL/I/ S junction—where “ I ” denotes the insulating “layer”—the repulsive e - e interaction results in a renormalization of the junction transparency

and the critical Josephson current is strongly suppressed.¹¹

Here we study the influence of the spin-orbit (SO) interaction on the Josephson current through a long S /I/LL/I/ S junction. The Luttinger-liquid part of the junction is represented by a quantum wire in a laterally confined 2DEG coupled to superconducting electrodes via tunnel barriers. It has been known for a long time that the SO interaction is strong in a 2DEG formed in a GaAs/AlGaAs inversion layer (the Rashba effect¹²) and that it can be controlled by a gate voltage.^{13–15} So the Rashba effect could strongly affect the superconducting properties of mesoscopic hybrid SN structures.¹⁶

The influence of the Rashba effect on the electron spectrum and on the transport properties of quasi-1D quantum wires has been studied theoretically in Refs. 17 and 18, where it was shown that the SO interaction not only splits the electron spectrum into “spin-up” and “spin-down” subbands, but additionally breaks the left-right symmetry. This implies that left- and right-moving electrons with the same spin projection have different Fermi velocities. Since, due to time invariance of the spin-orbit Hamiltonian $v_{R\uparrow}^{(F)} = v_{L\downarrow}^{(F)} = v_{1F}$ and $v_{R\downarrow}^{(F)} = v_{L\uparrow}^{(F)} = v_{2F}$, the strength of the Rashba effect in a single-channel QW can be characterized by a dispersion asymmetry parameter $\lambda_a = |v_{1F} - v_{2F}| / (v_{1F} + v_{2F})$. In Refs. 17 and 18 it was assumed that in the presence of the Rashba interaction the electron spins in a quasi-1D wire are aligned as in the 2D case (as indicated by the solid arrows in Fig. 1). Although this assumption is not valid for a strong Rashba coupling,¹⁹ the model considered in the cited references (see also Ref. 20) is interesting in itself. It allows one to study the effects of dispersion asymmetry ($\lambda_a \neq 0$) on the electron dynamics and in the limit $\lambda_a \rightarrow 0$ it reproduces the standard results for spin-1/2 electrons without the SO interaction.

Since the electron spin is not conserved in the presence of SO interactions the classification of spin states assumed in Refs. 17 and 18 is not evidently correct. Actually, as was shown in Ref. 19, it can be justified only for a weak Rashba

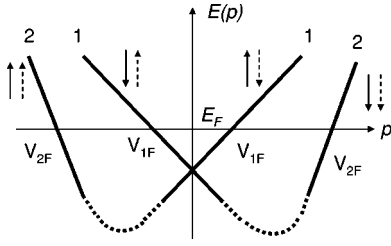


FIG. 1. Schematic energy spectrum of 1D spin-1/2 electrons with dispersion asymmetry. The subbands “1” and “2” are characterized by their Fermi velocities $v_{1F} \neq v_{2F}$. In the case of weak Rashba interaction, the spin projections for a given momentum have opposite directions in the two subbands (solid arrows). For strong Rashba interaction the spin projections are parallel for all particles that move in the same direction irrespective of subband, but are different for right- and left-moving particles (dashed arrows).

interaction. In the most interesting case of a strong Rashba interaction, when the characteristic energy scale introduced by the SO coupling is comparable with the energy spacing of the 1D subbands, the average spin projections for electrons with large (Fermi) momentum are different. The total energy is minimized when all right-moving (R) electrons have parallel spins pointing in the opposite direction to the spins of left-moving (L) electrons.¹⁹ In what follows we choose the sign of the Rashba interaction so that R electrons have their spin “down” and L electrons theirs “up” (as indicated by the dashed arrows in Fig. 1). Notice that under conditions when the Rashba effect is active the electron spin lies in a (2D) plane and orthogonal to the electron momentum (in the 1D case this direction is fixed and “up” and “down” spin projections are well defined).

At first we consider the influence of electron dispersion asymmetry on the superconducting properties of a $S/I/LL/I/S$ junction in the model elaborated in Refs. 17 and 18. In this model the spin projections of electrons in the leads are the same as in the wire and we can treat S/LL contacts as standard nonmagnetic scattering barriers. We calculate the Josephson current perturbatively using the junction transparency $D = |t_l t_r|^2$ as expansion parameter ($|t_{l,r}|^2 \ll 1$ are the transparencies of the tunnel barriers at the left and right LL/S interfaces) and for arbitrary values of electron-electron interaction strength, dispersion asymmetry λ_a and Zeeman splitting $\Delta_Z = g\mu_B B$ (g is the g factor, μ_B is the Bohr magneton, and B is the magnetic field). Two different geometries of $S/LL/S$ junction are considered. In the first case an effectively infinite LL is connected by the side electrodes to the bulk superconductors (“side-coupled” LL , see Fig. 2). In this geometry¹¹ one can use periodic boundary conditions for

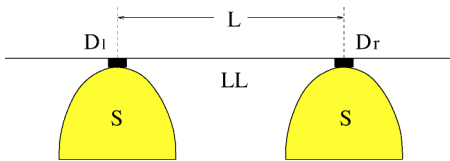


FIG. 2. $S/LL/S$ junction of length L formed by an effectively infinite Luttinger liquid coupled to bulk superconductors by side electrodes.

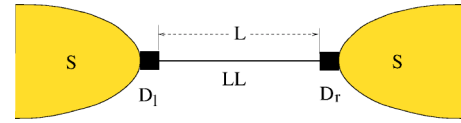


FIG. 3. A Luttinger-liquid wire of length L coupled to bulk superconductors via tunnel barriers with transparencies $D_{l(r)}$.

plasmons in the LL and all calculations can be done analytically even in the presence of SO interaction. When the dispersion asymmetry is negligibly small ($\lambda_a \rightarrow 0$) we reproduce the formula for the Josephson current derived in Ref. 11.

The interplay of electron dispersion asymmetry and the Zeeman interaction results in the appearance of an anomalous phase shift in the supercurrent, so that a supercurrent persists even in the absence of any phase difference between the two superconducting leads to which it is attached. The existence of this anomalous Josephson current is related to the breaking of chiral invariance in quasi-1D quantum wires^{17,18} and the effect manifests itself already for noninteracting particles (see Ref. 23).

A more realistic geometry for an $S/LL/S$ junction is a finite LL wire (of length L) coupled via tunnel barriers to bulk superconductors (“end-coupled” LL , see Fig. 3). We assume that the barrier transparencies are unequal and small (nonsymmetric tunnel junction) and evaluate the φ -dependent part of the ground-state energy by perturbation theory using the junction transparency D as expansion parameter. To first order in the junction transparency the problem is reduced to the evaluation of four-fermion correlation functions for a two channel LL Hamiltonian with the boundary conditions implying the absence of a particle current through the S/LL interfaces at $x=0, L$. In the absence of the spin-orbit interaction the problem of quantization of plasmon modes in a finite LL with open ends was solved in Ref. 24. Here, we generalize the quantization procedure proposed in the cited paper to the case of spin-1/2 fermions with dispersion asymmetry. We show that the spectrum of plasmons in a LL with open ends in the presence of dispersion asymmetry is determined by a transcendental equation. In the general case the spectrum forms a set of quasirandom energy levels. The plasmonic energies can not be separated into two independent set of levels—one for charge density excitations, another for spin density excitations. For noninteracting electrons, or when the energy dispersions are symmetric ($v_{1F} = v_{2F} = v_F$), the spectrum is reduced to a set of equidistant energy levels and the spin-charge separation is restored. In the limit of strongly interacting particles the plasmon spectrum also becomes regular. We calculate the Josephson current for the cases when the spectral equation can be solved analytically.

We find that a dispersion asymmetry affects the supercurrent only if the electron-electron interaction is weak. For noninteracting electrons the critical Josephson current through a tunnel $S/QW/S$ junction is enhanced by the presence of dispersion asymmetry. This behavior is specific for quasi-1D electrons and the effect disappears in 2D junctions.¹⁶

As has been already mentioned in this Introduction, the electron spin projections in a quasi-1D quantum wire in the

regime of strong Rashba effect are strongly correlated with the direction of electron motion and all right(left)-moving particles, irrespective of their Fermi velocities, have parallel spins¹⁹ which are antiparallel to the spin polarization of left(right)-moving electrons. So it is reasonable to expect that in this case the magnetic field via the Zeeman interaction will induce an anomalous phase shift even in the absence of dispersion asymmetry. At first we calculate the Josephson current in an adiabatic $S/LL/S$ junction when both the Rashba s - o interaction and the electrostatic confinement potential are smoothly switched on in a 1D QW. The anomalous Josephson current induced by a strong Zeeman interaction is predicted to be of the order of the critical current in adiabatic SNS junctions. For tunnel contacts the supercurrent is calculated in the limits of strong and weak e - e interaction. An anomalous phase shift of the Josephson current and an anomalous influence of the Zeeman splitting on the critical supercurrent is predicted. For noninteracting electrons we studied the influence of a strong Rashba effect on the resonant Josephson current through a symmetric $S/I/N/I/S$ junction and showed that the resonance effects survive only for special boundary conditions at NS interfaces.

The paper is organized as follows. Sections II–IV deal with the influence of an electron dispersion asymmetry on the proximity induced superconductivity in a LL wire. In Sec. II we calculate the Josephson current through a “side-coupled” LL wire. The spectrum of plasmonic modes in a LL with open ends and electron dispersion asymmetry is evaluated in Sec. III. In Sec. IV the Josephson current through an “end-coupled” LL wire is analytically calculated in the limits of weak and strong electron-electron interaction. In Sec. V we consider the regime of strong Rashba interaction and analytically evaluate the Josephson current in the “end-coupled” LL wire in the limits of strong and weak e - e interaction. The results obtained are summarized in Sec. VI.

II. PROXIMITY-INDUCED SUPERCONDUCTIVITY IN A LUTTINGER LIQUID WIRE WITH ASYMMETRY OF ELECTRON DISPERSIONS

It is physically evident that the Coulomb interaction in a long $S/I/LL/I/S$ junction suppresses the critical supercurrent due to a strong Kane-Fisher renormalization of the bare tunneling matrix elements. The Josephson current through a Luttinger liquid coupled to bulk superconductors via tunnel contacts was first calculated by Fazio *et al.*¹¹ who showed that the critical supercurrent is multiplicatively renormalized (suppressed) by a repulsive electron-electron interaction. The calculations were performed in linear (Fig. 2) and ringlike geometries. In both cases periodic boundary conditions for the plasmonic modes can be imposed. Although from an experimental point of view the considered geometries of an SNS junction look rather artificial, they do allow one to simplify the calculations.

For noninteracting electrons the critical supercurrents in an SNS junction formed by a long (effectively infinite) quantum wire connected to superconductors by side tunnel contacts (separated by a distance L) and in an SNS junction where a finite length QW bridges the gap (of the same length

L) between two superconductors differ only by a numerical factor. If the QW is treated as a Luttinger liquid this factor becomes a function of the interaction strength and can be evaluated analytically (see below). When both electron-electron interactions and dispersion asymmetry are present the calculations are more cumbersome. We start with the case of a side-contacted QW where we are able to analytically evaluate the supercurrent for arbitrary interaction strength and dispersion asymmetry parameter.

The Hamiltonian $H=H_{LL}+H_b$ of a $S/I/LL/I/S$ junction is a sum of the LL Hamiltonian H_{LL} and the boundary Hamiltonian H_b . The latter describes the effective boundary pairing and scattering interactions produced by the superconducting and normal scattering potentials at the points $x=0$ and $x=L$ (see Ref. 27). In the presence of an electron dispersion asymmetry the corresponding spin-1/2 LL Hamiltonian expressed in terms of charge densities of chiral fields takes the form

$$H_{LL} = \pi\hbar \int dx \left\{ u_1(\rho_{R\uparrow}^2 + \rho_{L\downarrow}^2) + u_2(\rho_{R\downarrow}^2 + \rho_{L\uparrow}^2) + \frac{V_0}{\pi\hbar} (\rho_{R\uparrow}\rho_{R\downarrow} + \rho_{L\uparrow}\rho_{L\downarrow} + \rho_{R\uparrow}\rho_{L\uparrow} + \rho_{R\downarrow}\rho_{L\downarrow} + \rho_{R\downarrow}\rho_{L\downarrow} + \rho_{R\uparrow}\rho_{L\downarrow} + \rho_{R\downarrow}\rho_{L\uparrow}) \right\}, \quad (1)$$

where $\rho_{R/L,\uparrow/\downarrow}$ are the charge density operators of right/left-moving electrons with up/down-spin projection, V_0 is the strength of electron-electron interaction ($V_0 \sim e^2$), and $u_{1(2)} = v_{1(2)F} + V_0/2\pi\hbar$. The Fermi velocities $v_{1F} \neq v_{2F}$ are different due to an assumed electron dispersion asymmetry (see Fig. 1). We have neglected the magnetic field-induced corrections to the Fermi velocities and assumed that the effective electron-electron interaction has no significant magnetic field dependence. Both the neglected effects are of “ $1/\varepsilon_F$ ” order (see, e.g., Ref. 28) and they are irrelevant for Zeeman splittings $\Delta_Z \ll |\Delta| \ll \varepsilon_F$.

The Hamiltonian (1) is equivalent to a two-channel LL Hamiltonian and can be diagonalized by the canonical transformation suggested in Ref. 25 (see Appendix). The diagonalized Hamiltonian is

$$H_d = \pi\hbar \int dx \{ s_1(\rho_{R1}^2 + \rho_{L1}^2) + s_2(\rho_{R2}^2 + \rho_{L2}^2) \}, \quad (2)$$

where $s_{(1,2)}$ are the velocities of noninteracting bosonic modes (see the Appendix).

We assume strong normal backscattering at the S/N boundaries (tunnel junctions). In this limit the pairing Hamiltonian contains a small factor—the amplitude of Andreev backscattering^{29,30}

$$r_A^{(r,l)} \simeq D_{r,l} \exp \left[i \left(\frac{\pi}{2} + \varphi_{r,l} \right) \right], \quad (3)$$

where $D_{r(l)} \ll 1$ is the transparency of the barrier at the right-(left) interface, $\varphi_{r(l)}$ is the phase of the superconducting order parameter on the right(left) bank of the junction. The boundary Hamiltonian for our two-channel system can be expressed in terms of the Andreev scattering amplitudes Eq. (3) up to an overall numerical factor C , which will be specified later

$$\begin{aligned}
H_b/C &= \hbar v_{1F} [r_A^{*(l)} \Psi_{R\uparrow}(0) \Psi_{L\downarrow}(0) - r_A^{*(r)} \Psi_{R\uparrow}(L) \Psi_{L\downarrow}(L)] \\
&+ \hbar v_{2F} [r_A^{*(l)} \Psi_{R\downarrow}(0) \Psi_{L\uparrow}(0) - r_A^{*(r)} \Psi_{R\downarrow}(L) \Psi_{L\uparrow}(L)] \\
&+ \text{H.c.}
\end{aligned} \quad (4)$$

To second order in the Andreev scattering amplitude the phase dependent part of the ground-state energy takes the form

$$\delta E^{(2)}(\varphi) = \sum_j \frac{| \langle j | H_b | 0 \rangle |^2}{E_0 - E_j} = \frac{1}{\hbar} \int_0^\infty d\tau \langle 0 | H_b^\dagger(\tau) H_b(0) | 0 \rangle, \quad (5)$$

where $H_b(\tau)$ is the boundary Hamiltonian (4) in the imaginary time Heisenberg representation. After substituting Eq. (4) into Eq. (5) we get the following expression for $\delta E^{(2)}(\varphi)$ expressed in terms of electron correlation functions:

$$\begin{aligned}
\delta E^{(2)}(\varphi) &= -4C\hbar \text{Re} \left\{ r_A^{*(l)} r_A^{(r)} \int_0^\infty d\tau [v_{1F}^2 \langle \Psi_{R\uparrow}(\tau, 0) \Psi_{L\downarrow}(\tau, 0) \right. \\
&\quad \left. \times \Psi_{L\downarrow}^\dagger(0, L) \Psi_{R\uparrow}^\dagger(0, L) \rangle + v_{2F}^2 \langle \uparrow \leftrightarrow \downarrow \rangle] \right\}. \quad (6)
\end{aligned}$$

We will calculate the electron correlation functions in Eq. (6) by making use of the bosonization technique. Notice that the Zeeman splitting introduces an extra x -dependent phase factor in the chiral components of the fermion fields. This interaction can be taken into account (see, e.g., Ref. 20) by replacing the fermion operators in Eq. (6) by $\Psi_{\mu, \sigma}^{(Z)}$, where

$$\Psi_{\mu, \sigma}^{(Z)} = \exp(iK_Z x) \Psi_{\mu, \sigma}, \quad K_Z = \frac{\Delta_Z}{4\hbar v_F} \frac{\mu\sigma - \lambda_a}{1 - \lambda_a^2}, \quad (7)$$

Here $v_F = (v_{1F} + v_{2F})/2$, $\mu = (R, L) \equiv (1, -1)$, $\sigma = (\uparrow, \downarrow) \equiv (1, -1)$, Δ_Z is the Zeeman splitting, and $\lambda_a = (v_{1F} - v_{2F})/(v_{1F} + v_{2F})$ is the parameter which characterizes the strength of chiral symmetry breaking.

The standard bosonization formulae now read

$$\begin{aligned}
\Psi_{R(L), \uparrow}(x, t) &= \frac{\exp\{\pm i\sqrt{4\pi}\Phi_{R(L), \uparrow}(x, t)\}}{\sqrt{2\pi a_{1(2)}}}, \\
\Psi_{R(L), \downarrow}(x, t) &= \frac{\exp\{\pm i\sqrt{4\pi}\Phi_{R(L), \downarrow}(x, t)\}}{\sqrt{2\pi a_{2(1)}}}, \quad (8)
\end{aligned}$$

where $a_{1,2}$ are the cutoff parameters of the two-channel LL. The chiral bosonic fields in Eq. (8) for a finite length LL are represented as follows (see, e.g., Ref. 31)

$$\Phi_{R(L), \uparrow}(x, t) = \frac{1}{2} \hat{\Phi}_{R(L), \uparrow} + \hat{\Pi}_\uparrow \frac{x \mp v_{1(2)} t}{L_{1(2)}} + \varphi_{R(L), \uparrow}(x, t), \quad (9)$$

$$\Phi_{R(L), \downarrow}(x, t) = \frac{1}{2} \hat{\Phi}_{R(L), \downarrow} + \hat{\Pi}_\downarrow \frac{x \mp v_{2(1)} t}{L_{2(1)}} + \varphi_{R(L), \downarrow}(x, t). \quad (10)$$

Here the zero mode operators ($\hat{\Phi}_{R(L), \sigma}$, $\hat{\Pi}_{\sigma'}$) obey the commutation relations $[\hat{\Phi}_{R(L), \sigma}, \hat{\Pi}_{\sigma'}] = \mp i\delta_{\sigma, \sigma'}$ and the non-topological (harmonic) components $\varphi_{R(L), j}(x, t)$ are

$$\varphi_{R(L), j}(x, t) = \sum_q \sqrt{\frac{1}{2qL_j}} \{e^{iq(\pm x - v_j t)} \hat{b}_q + \text{H.c.}\}, \quad (11)$$

where b_q (b_q^\dagger) are the standard bosonic annihilation (creation) operators. The effective quantization lengths L_j ($j=1, 2$) depend on the boundary conditions and will be specified in the next section.

As is well known (see, e.g., Ref. 32), the topological excitations for an effectively infinite LL play no role and can be omitted in Eqs. (9) and (10). After straightforward transformations Eq. (6) is reduced to the following expression:

$$\begin{aligned}
\delta E^{(2)}(\varphi) &= 4C\hbar D \left\{ v_{1F}^2 \cos\left(\varphi - \frac{\Delta_Z}{\Delta_{1L}}\right) \int_0^\infty d\tau \Pi_1(\tau) \right. \\
&\quad \left. + v_{2F}^2 \cos\left(\varphi + \frac{\Delta_Z}{\Delta_{2L}}\right) \int_0^\infty d\tau \Pi_2(\tau) \right\}, \quad (12)
\end{aligned}$$

where $D = D_l D_r$ is the junction transparency, $\Delta_{1(2)L} = \hbar v_{1(2)F}/L$ and

$$\begin{aligned}
\Pi_{1(2)}(\tau) &= \frac{1}{(2\pi a_{1(2)})^2} \exp\{2\pi i [\langle \varphi_\sigma(\tau, -L) \varphi_\sigma \rangle \\
&\quad + \langle \langle \Theta_\rho(\tau, -L) \Theta_\rho \rangle \rangle \pm \langle \langle \Theta_\rho(\tau, -L) \varphi_\sigma \rangle \rangle \\
&\quad \pm \langle \langle \varphi_\sigma(\tau, -L) \Theta_\rho \rangle \rangle] \}. \quad (13)
\end{aligned}$$

Here $\varphi_\sigma \equiv \varphi_\sigma(0, 0)$, $\Theta_\rho \equiv \Theta_\rho(0, 0)$ and double brackets denote the subtraction of the corresponding vacuum average at the points $\tau, x=0$. The charge (ρ) and spin (σ) bosonic fields in Eq. (13) are related to the chiral fields $\varphi_{R(L), \uparrow(\downarrow)}$ introduced above by the simple linear equations

$$\varphi_\sigma(\Theta_\rho) = \frac{1}{\sqrt{2}} (\varphi_{R, \uparrow} \pm \varphi_{L, \uparrow} \mp \varphi_{R, \downarrow} - \varphi_{L, \downarrow}) \quad (14)$$

(the upper sign corresponds to φ_σ and the lower sign denotes Θ_ρ). With the help of the canonical transformation Eq. (A1) the chiral bosonic fields in Eq. (14) can be expressed in terms of noninteracting plasmonic modes $\varphi_{R/L, j}$ ($j=1, 2$). For an infinitely long LL the propagators of these fields are (see, e.g., Ref. 32)

$$\langle \langle \varphi_{R/L, j}(t, x) \varphi_{R/L, k} \rangle \rangle = -\frac{\delta_{jk}}{4\pi} \ln \frac{a_k \mp x + is_k t}{a_k}, \quad (15)$$

where the velocities s_j are defined in the Appendix [see Eqs. (A4) and (A5)]. Finally, the expression for the Josephson current through a side-coupled LL wire (Fig. 2) takes the form

$$\begin{aligned}
 J^{(i)}(V_0, \lambda_a, \Delta_Z; \varphi) &= \frac{eV_F}{L} D \frac{C}{2\pi^2} \left\{ \left(\frac{a_1}{L} \right)^{2(\gamma_1-1)} \frac{v_{1F}^2}{s_1 v_F} B(1/2, \gamma_1 - 1/2) \right. \\
 &\quad \times F(1/2, \gamma_{1s}; \gamma_1; 1 - (s_2/s_1)^2) \\
 &\quad \times \sin\left(\varphi - \frac{\Delta_Z}{\Delta_{1L}}\right) + \left(\frac{a_2}{L} \right)^{2(\gamma_2-1)} \\
 &\quad \times \frac{v_{2F}^2}{s_1 v_F} B(1/2, \gamma_2 - 1/2) F(1/2, \gamma_{2c}; \gamma_2; 1 - (s_2/s_1)^2) \\
 &\quad \left. \times \sin\left(\varphi + \frac{\Delta_Z}{\Delta_{2L}}\right) \right\}, \quad (16)
 \end{aligned}$$

where $B(x, y) = \Gamma(x)\Gamma(y)/\Gamma(x+y)$ is the beta function, $F(\alpha, \beta; \gamma; z)$ is the hypergeometric function (see, e.g., Ref. 26), $v_F = (v_{1F} + v_{2F})/2$, $\gamma_j = \gamma_{js} + \gamma_{jc}$ ($j=1, 2$), and

$$\begin{aligned}
 \gamma_{1s} &= \frac{v_{2F}}{v_{1F}} \frac{\sin^2 \psi}{g_2}, & \gamma_{1c} &= \frac{\cos^2 \psi}{g_1}, \\
 \gamma_{2s} &= \gamma_{1s} (1 \leftrightarrow 2), & \gamma_{2c} &= \gamma_{1c} (1 \rightarrow 2). \quad (17)
 \end{aligned}$$

Here $g_j = s_j/v_{jF}$ are the correlation parameters of a two-channel LL (see the Appendix) and angle parameter ψ is defined by Eq. (A3).

By using the properties of the hyper-geometric function it is easy to show that for a given strength of the electron-electron interaction the Josephson current $J^{(i)}$ satisfies the equations

$$J^{(i)}(-\lambda_a, \Delta_Z; \varphi) = J^{(i)}(\lambda_a, -\Delta_Z; \varphi) = -J^{(i)}(\lambda_a, \Delta_Z; -\varphi) \quad (18)$$

which describe the symmetries of electric current with respect to space and time reflections. In particular one can infer from Eq. (18) that when both the dispersion asymmetry ($\lambda_a \neq 0$) and the Zeeman ($\Delta_Z \neq 0$) interaction are present the supercurrent could be nonzero even at $\varphi=0$. This anomalous supercurrent exists already for noninteracting electrons ($V_0=0$) and at first we analyze Eq. (16) in the limit of weak e - e interaction.

For noninteracting electrons ($V_0=0$, $g_1=g_2=1$) Eq. (16) is much simplified to

$$J_0^{(i)}(\varphi) = J_c^{(0)} \frac{1}{2} \left\{ \frac{v_{1F}}{v_F} \sin\left(\varphi - \frac{\Delta_Z}{\Delta_{1L}}\right) + \frac{v_{2F}}{v_F} \sin\left(\varphi + \frac{\Delta_Z}{\Delta_{2L}}\right) \right\}, \quad (19)$$

where $J_c^{(0)} = (Dev_F/4L)(C/\pi)$ is the critical Josephson current. We see that in the absence of magnetic interaction ($\Delta_Z=0$) the Rashba interaction in the considered geometry of SNS junction does not affect Josephson current at all (see also Ref. 16 where an analogous result was obtained for a short 2D SNS junction in the presence of Rashba spin-orbit interaction). The interplay of the Zeeman interaction and the dispersion asymmetry in quantum wires results in the appearance of an anomalous (at $\varphi=0$) Josephson current $J_a^{(i)} \equiv J_0^{(i)}(\varphi=0)$ which it is convenient to express in terms of the

asymmetry parameter λ_a and the magnetic phase $\chi_B = \Delta_Z/\Delta_L$ ($\Delta_L = \hbar v_F/L$) as

$$\begin{aligned}
 J_a^{(i)}(\lambda_a, \chi_B) &= \frac{J_c^{(0)}}{2} \left\{ (1 - \lambda_a) \right. \\
 &\quad \left. \times \sin\left(\frac{\chi_B}{1 - \lambda_a}\right) - (1 + \lambda_a) \sin\left(\frac{\chi_B}{1 + \lambda_a}\right) \right\}. \quad (20)
 \end{aligned}$$

As is evident from the above equation, the anomalous supercurrent J_a appears only when both the dispersion asymmetry and the Zeeman interaction are present $J_a(\lambda_a=0, \Delta_Z) = J_a(\lambda_a, \Delta_Z=0) = 0$. In the limit of weak dispersion asymmetry $\lambda_a \ll 1$ (a realistic case¹⁷ for quantum wires formed in 2DEG) the Josephson current as a function of Zeeman splitting demonstrates a simple harmonic²¹ behavior with a slow periodically varying amplitude (beats)

$$J_0^{(i)} \simeq J_c^{(0)} \sin(\varphi + \delta\varphi_a) \cos\left(\frac{\Delta_Z}{\Delta_L}\right), \quad \delta\varphi_a = \lambda_a \left(\frac{\Delta_Z}{\Delta_L} - \tan \frac{\Delta_Z}{\Delta_L} \right). \quad (21)$$

This formula clearly demonstrates that the interplay of a weak Rashba interaction and the Zeeman interaction results in anomalous phase shift $\delta\varphi$ in the supercurrent. In what follows we will see that for a strong Rashba interaction the analogous phase shift is determined mostly by Zeeman splittings and is finite even for symmetric electron dispersions.

Now we analyze Eq. (16) in the limit when dispersion asymmetry is negligibly small ($\lambda_a=0$). In this case the Josephson current through the LL wire takes the form

$$J^{(i)} = J_c^{(g)} \cos \chi_B \sin \varphi, \quad J_c^{(g)} = R(g_c) J_c^{(0)}, \quad (22)$$

where the interaction-induced renormalization factor $R(g_c)$ (here $g_c^{-1} = \sqrt{1 + 2V_0/\pi\hbar v_F}$ is the LL correlation parameter in the charge sector)

$$R(g_c) = \frac{g_c}{\sqrt{\pi} \Gamma(1/2 + 1/2g_c)} F\left(\frac{1}{2}, \frac{1}{2}; \frac{1}{2g_c} + \frac{1}{2}; 1 - g_c^2\right) \left(\frac{a}{L}\right)^{g_c^{-1}-1} \quad (23)$$

is equivalent to the one evaluated in Ref. 11 (in the cited paper this factor was presented in the integral form). In the limit of strong interaction $V_0/\hbar v_F \gg 1$ the renormalization factor is small

$$R(g_c \ll 1) \simeq \frac{\pi}{2} \left(\frac{\hbar v_F}{V_0} \right)^{3/2} \left(\frac{a}{L} \right)^{\sqrt{2V_0/\pi\hbar v_F}} \ll 1 \quad (24)$$

and the Josephson current through a $S/I/LL/I/S$ junction is strongly suppressed.¹¹

When both the electron-electron interaction and the dispersion asymmetry are strong, only one of the two terms in Eq. (16) dominates. The corresponding critical current (for definiteness we assume that $v_{1F} \simeq v_F/2 \gg v_{2F}$)

$$J_c^{(i)} = J_c^{(0)} \pi \left(\frac{\hbar v_{1F}}{V_0} \right)^{3/2} \left(\frac{a}{L} \right)^{2\sqrt{V_0/\pi\hbar v_{1F}}} \quad (25)$$

is much smaller than the critical current J_c in the absence of dispersion asymmetry ($v_{1F}=v_{2F}$). It means that dispersion asymmetry in quantum wires could enhance the interaction-induced suppression of the Josephson current. Notice, however, that the considered model of spin-orbit interaction in quasi-1D wires^{17,18} is not valid when the Rashba effect is strong. So in reality the enhancement induced by a weak electron dispersion asymmetry is small.

III. DISPERSION ASYMMETRY AND QUASI-RANDOM ENERGY SPECTRUM OF PLASMONS

In this section we evaluate the spectrum of topological excitations and plasmonic modes in a LL wire of the length L end-coupled to bulk superconductors (see Fig. 3). The electron normal backscattering at the N/S interfaces is assumed to be strong. The Josephson current can be calculated to the first order on junction transparency using Eq. (6) for the φ dependent part of the ground-state energy. For a finite length LL the zero modes in Eqs. (9) and (10) contribute to the energy and after some algebra we get for $\delta E^{(2)}(\varphi)$ an expression analogous to Eq. (12) where now $\Pi_{1(2)}(\tau)$ is replaced by the product $\Pi_{1(2)}(\tau)Q_{1(2)}(\tau)$. The zero mode contributions $Q_{1(2)}(\tau)$ are ($j=1, 2$)

$$Q_j(\tau) = \exp \left\{ -2\pi \left\langle \left[\frac{L}{L_j} (\hat{\Pi}_\uparrow - \hat{\Pi}_\downarrow) + \frac{iv_j\tau}{L_j} (\hat{\Pi}_\uparrow + \hat{\Pi}_\downarrow) \right]^2 \right\rangle \right\} \times \exp \left(\frac{2\pi v_j\tau}{L_j} \right). \quad (26)$$

To zeroth order of perturbation theory in the barrier transparencies the electrons are confined to the normal region. Therefore the correlation functions in Eq. (12) have to be calculated with the appropriated boundary conditions. The natural boundary condition for our problem is the requirement that the particle current through the interfaces at $x=0, L$ is zero

$$J_\sigma \sim \text{Re} \{ i\Psi_\sigma^\dagger \partial_x \Psi_\sigma \}_{x=0,L} = 0, \quad \sigma = \uparrow, \downarrow. \quad (27)$$

Here the wave function Ψ_σ for the nonsymmetric electron dispersion is represented as

$$\Psi_{\uparrow(L)} \simeq e^{ik_{1(2)F}x} \Psi_{R1(2)}(x) + e^{-ik_{2(1)F}x} \Psi_{L(2)1}(x). \quad (28)$$

Notice that Eqs. (27) and (28) determine more general boundary conditions than $\Psi_\sigma(x=0, L)=0$ usually assumed in the literature (see, e.g., Ref. 22). The last b.c. is the particular case of so called ‘‘hard wall’’ b.c.’s $\Psi^{(j)}(x_b)=0$ $j=1, \dots, 2N$ for a multichannel (N) spin-1/2 LL. They do not mix the channels and allows one to reduce the multichannel problem to calculations for a single channel situation with an additional summation of channel-dependent quantities over channel quantum numbers.²² In our case scattering at the boundaries changes the channel ‘‘index’’ ($1 \leftrightarrow 2$) and the correct b.c. for ‘‘slow’’ fields $\Psi_{R(L)}$ has to take this fact into account. The decomposition Eq. (28) holds at distances much larger

than λ_F . In a general case, the wave function at the boundary is of a more complicated (and unknown) form and one may not put $\Psi_\sigma=0$ in order to find the relations between the two terms in Eq. (28). In contrast, the requirement that the particle current through the boundary is zero is robust and its consequences hold at any distance from the boundary due to current conservation.

For the bare electron spectrum without dispersion asymmetry ($k_{1F}=k_{2F}=k_F$) the formulated requirement is equivalent to the following boundary conditions for the chiral(R,L) fermionic fields (see also Ref. 24):

$$\Psi_{R\sigma}^\dagger(x) \Psi_{R\sigma}(x)_{x=0,L} = \Psi_{L\sigma}^\dagger(x) \Psi_{L\sigma}(x)_{x=0,L}. \quad (29)$$

The boundary conditions Eq. (29) correspond to a LL with open ends²⁴ and result in zero eigenvalues of the momentum-like zero-mode operator $\hat{\Pi}_\sigma$ and in quantization of harmonic modes (plasmons) on a ring with circumference $2L$ (see Ref. 24). In this case the spectrum of plasmons is equidistant and the propagators take the form ($j, k=1, 2$)

$$\langle \langle \varphi_{R(L)j}(t, x) \varphi_{R(L)k} \rangle \rangle = -\frac{\delta_{jk}}{4\pi} \ln \frac{1 - \exp[i\pi(\pm x - s_k t + ia)/L]}{\pi a/L}. \quad (30)$$

Here a is the cutoff length and $s_{1(2)}$ are the velocities of charge and spin excitations (for noninteracting fermions $s_1 = s_2 = v_F$).

Now we generalize the quantization procedure elaborated in Ref. 24 to an electron spectrum with dispersion asymmetry. We will assume that electron normal backscattering at the boundaries is not accompany by spin-flip processes. Therefore each backscattering for our spectrum (Fig. 1) leads to the change of the channel index (‘‘1’’ \leftrightarrow ‘‘2’’) and the corresponding Fermi velocity.

It is worthwhile at first to consider the general case of boundary scattering in a two-channel system of noninteracting electrons confined to the interval $[0, L]$. The electron backscattering at the boundaries is described by 2×2 unitary symmetric matrix which is convenient to parametrize as follows:

$$\hat{S} = e^{i\delta} \begin{pmatrix} r & i|t| \\ i|t| & r^* \end{pmatrix}, \quad (31)$$

where $r = |r|e^{i\delta_r}$ is the intrachannel backscattering amplitude ($1 \leftrightarrow 1, 2 \leftrightarrow 2$) and t is the interchannel backscattering ($1 \leftrightarrow 2$) amplitude $|r|^2 + |t|^2 = 1$. By matching the electron wave functions at the boundaries $x=0$ and $x=L$ with the help of the S -matrix Eq. (31) one easily finds the spectrum equation

$$\cos^2 \left[\frac{\varepsilon L}{2} \left(\frac{1}{v_{1F}} + \frac{1}{v_{2F}} \right) + \delta \right] = |r|^2 \cos^2 \left[\frac{\varepsilon L}{2} \left(\frac{1}{v_{1F}} - \frac{1}{v_{2F}} \right) + \delta_r \right]. \quad (32)$$

For purely intrachannel reflection, $t=0$, we get from Eq. (32) two independent sets ($j=1, 2$) of equidistant levels with spacing $\Delta \varepsilon_j = \pi \hbar v_{jF}/L$. In the opposite case of purely interchannel backscattering ($r=0$) the spectrum is also equidistant

$$\varepsilon_n = \frac{2\pi\hbar}{L} \frac{v_{1F}v_{2F}}{v_{1F}+v_{2F}} \left(n + \frac{1}{2} - \frac{\delta}{\pi} \right), \quad n = 1, 2, \dots \quad (33)$$

In a general case the spectral equation (32) yields a set of quasirandom energy levels.

The bozonization technique is efficient only for the two considered limiting cases: $|r|=1$ (this was demonstrated in Ref. 24), and $r=0$ as we will show now. Let us start at first with the case on noninteracting fermions. The boundary condition Eq. (27) for $v_{1F} \neq v_{2F}$ results in the equations

$$v_{1F} \Psi_{R1}^\dagger(x) \Psi_{R1}(x)|_{x=0,L} = v_{2F} \Psi_{L2}^\dagger(x) \Psi_{L2}(x)|_{x=0,L}, \quad (34)$$

$$\text{Re}[\Psi_{L2}^\dagger(x) \Psi_{R1}(x) e^{i(k_{1F}+k_{2F})x}]_{x=0,L} = 0. \quad (35)$$

These equations are satisfied if

$$\frac{a_1}{a_2} = \frac{L_1}{L_2} = \frac{v_{1F}}{v_{2F}}, \quad \frac{1}{L_1} + \frac{1}{L_2} = \frac{1}{L}, \quad (36)$$

$$\varepsilon_n^F = \frac{2\pi}{L} \frac{v_{1F}v_{2F}}{v_{1F}+v_{2F}} n, \quad n = 1, 2, \dots, \quad (37)$$

and

$$[\Phi_{L\sigma}(x,t) + \Phi_{R\sigma}(x,t)]_{x=0,L} = \frac{\sqrt{\pi}}{2} n_\sigma, \quad \sigma = \uparrow, \downarrow, \quad (38)$$

where n_\uparrow and n_\downarrow are integers. Eq. (38) in its turn is satisfied for topological sector with quantum numbers $(\hat{\varphi}_{R\sigma} + \hat{\varphi}_{L\sigma})/\sqrt{\pi} = n_\sigma$, $\hat{\Pi}_\sigma = 0$ and the harmonic modes $\varphi_{R(L)\sigma}(x,t)$ which obey the relations

$$\varphi_{R\sigma}(x,t)_{x=0,L} = -\varphi_{L\sigma}(x,t)_{x=0,L}. \quad (39)$$

From Eqs. (11), (36), and (39) one easily gets the plasmon spectrum

$$\varepsilon_n = \frac{2\pi}{L} \frac{s_1 s_2}{s_1 + s_2} n \quad (40)$$

($s_{1,2}$ are the plasmon velocities, which coincide with the Fermi velocities for noninteracting fermions) and the desired correlation functions ($j, k=1, 2$)

$$\langle\langle \varphi_{R(L)j}(x,t) \varphi_{R(L)k} \rangle\rangle = -\frac{\delta_{jk}}{4\pi} \ln \frac{1 - \exp[i2\pi(\pm x - s_k t + i a_k)/L_k]}{2\pi a_k/L_k}, \quad (41)$$

where the effective quantization lengths L_j according to Eq. (36) are

$$L_{1(2)} = \frac{v_{1F} + v_{2F}}{v_{2(1)F}} L. \quad (42)$$

In the limit $v_{1F} = v_{2F}$ Eqs. (40)–(42) reproduce the plasmon spectrum and the correlation functions of a single channel LL with open ends.²⁴

Now we are ready to consider the effects of interaction. For a single-mode LL (or for a multichannel LL, provided the backscattering does not mix the channels) the boundary condition Eq. (39) for harmonic modes holds also for inter-

acting fermions as one can check using a Bogoliubov-like transformation which diagonalizes the LL Hamiltonian. Hence in the presence of interaction one can still use the same correlation functions as for noninteracting fermions with the only difference that the velocities are renormalized by interaction.

This is not the case for our problem. With the help of exact transformations [see the Appendix, Eq. (A1)] which diagonalize the 2-channel LL Hamiltonian²⁵ one can show that if the chiral bosonic fields satisfy Eq. (39), the diagonalized ones $\tilde{\varphi}_{R(L)j}$ are connected at the boundaries by the effective ‘‘scattering matrix’’ \hat{S}^e

$$\tilde{\varphi}_{Rj}(x=0,L) = \sum_{k=1}^{k=2} S_{jk}^e \tilde{\varphi}_{Lk}(x=0,L), \quad \hat{S}^e = \frac{1}{B} \begin{pmatrix} -A & 1 \\ 1 & A \end{pmatrix}, \quad (43)$$

where the coefficients A, B are

$$A = -[\cos 2\psi - \sinh(\vartheta_1 - \vartheta_3) \sin 2\psi]^{-1} [\sinh(\vartheta_1 - \vartheta_2) \times \cosh(\vartheta_1 - \vartheta_3) + \cos 2\psi \cosh(\vartheta_1 - \vartheta_2) \sinh(\vartheta_1 - \vartheta_3) + \sin 2\psi \cosh(\vartheta_1 - \vartheta_2)], \quad (44)$$

$$B = -[\cos 2\psi - \sinh(\vartheta_1 - \vartheta_3) \sin 2\psi]^{-1} [\cosh(\vartheta_1 - \vartheta_2) \times \cosh(\vartheta_1 - \vartheta_3) + \cos 2\psi \sinh(\vartheta_1 - \vartheta_2) \sinh(\vartheta_1 - \vartheta_3) + \sin 2\psi \sinh(\vartheta_1 - \vartheta_2)] \quad (45)$$

and the ‘‘rotation angles’’ ϑ_l ($l=1, \dots, 4$) and ψ are defined in the Appendix [see Eqs. (A2) and (A3)]. One can check after some algebra that the coefficients A and B satisfy the simple relation $B^2 - A^2 = 1$, which makes the S matrix in Eq. (43) unitary. This observation allows us to use the scattering matrix formalism when evaluating the energy spectrum of plasmons. Notice that in the parametrization Eq. (31) we have $r = iA/B$, $|t| = 1/B$, $\delta = \pi/2$.

For monochromatic bosonic fields with amplitudes $b_{R(L)j}$ the scattering at the boundaries $x=0$ and $x=L$ are determined by the equations

$$x=0: b_{Rj} = \sum_{k=1}^2 S_{jk}^e b_{Lk}, \quad x=L: e^{-i\alpha_j} b_{Lj} = \sum_{k=1}^2 S_{jk}^e e^{i\alpha_k} b_{Rk}, \quad (46)$$

where the phases $\alpha_j = \varepsilon L/s_j$ and s_j are the plasmon velocities [see Eqs. (A4) and (A5)]. From the above set of linear equations one easily finds the spectrum equation for plasmons

$$\sin^2 \left[\frac{\varepsilon L}{2} \left(\frac{1}{s_1} + \frac{1}{s_2} \right) \right] = R \sin^2 \left[\frac{\varepsilon L}{2} \left(\frac{1}{s_1} - \frac{1}{s_2} \right) \right], \quad (47)$$

where $R \equiv (A/B)^2 \leq 1$ is the effective backscattering coefficient for plasmons. It depends both on the dimensionless interaction strength $\kappa = V_0/\pi\hbar(v_{1F}+v_{2F})$ and on the dispersion asymmetry parameter λ_a . Notice that the spectral equation (47) is the special case of Eq. (32) for $\delta = \delta_r = \pi/2$.

The derived spectral equation has simple exact analytic solutions in two limiting cases: (i) noninteracting fermions and (ii) when dispersion asymmetry is absent, $v_{1F} = v_{2F} = v_F$.

For noninteracting particles [$V_0=0$ in Eq. (1)] the “rotation angles” are $\psi=0$, $\vartheta_1=\vartheta_4=0$ (see the Appendix) and the velocities $s_1=v_{1F}$, $s_2=v_{2F}$. Then $A=0$, $B=-1$ and the effective backscattering coefficient $R=0$. Eq. (47) in this limit reproduces the equidistant spectrum of “noninteracting” plasmons, Eq. (33). For interacting fermions in the absence of dispersion asymmetry the “rotation angles” are $\vartheta_1=\vartheta_3$, $\vartheta_2=\vartheta_4$, $\cos 2\psi=0$. In this limit $s_1=s$, $s_2=v_F$ and $R=1$. The corresponding plasmon energies $\varepsilon_n^{(1)}=\pi sn/L$, $\varepsilon_n^{(2)}=\pi v_F n/L$, ($n=1, 2, \dots$) represent the standard excitations in the charge and spin sector of a finite length (L) Luttinger liquid with open ends.²⁴

For a general case Eq. (47) has to be solved numerically and the plasmon spectrum represents a set of quasirandom energy levels. Now the plasmonic energies cannot be separated into independent sets of levels for charge and spin density excitations. It means that the considered boundary conditions strongly mix the charge and spin excitations and the phenomena of charge-spin separation, well known in a LL, strictly speaking, disappears when both spin-orbit interaction and finite size effects are present.

IV. JOSEPHSON CURRENT THROUGH A FINITE-LENGTH LL WIRE WITH DISPERSION ASYMMETRY

It is clear from a physical point of view that the effects of a dispersion asymmetry in the bare electron spectrum have to be most significant in the quantum dynamics of noninteracting electrons. In this case the mismatch in Fermi velocities when an electron is backscattered at the boundaries leads to an intricate interference pattern. The more strongly particles interact, the less important are the effects of dispersion asymmetry. For instance, in the limiting case of a 1D Wigner crystal (strong repulsive long-range interactions) it is hard to imagine any interference produced by the quantum dynamics of plasmons in two Wigner crystals pinned by structural imperfections at the boundaries. So in our problem it is reasonable to expect the restoration of the regular plasmon spectrum and the spin-charge separation in the limit of strong interaction.

For strongly interacting electrons $\kappa=V_0/\pi\hbar(v_{1F}+v_{2F}) \gg 1$ and $v_{1F} \sim v_{2F}$ (i.e., for a realistic case of weak or moderate dispersion asymmetry) the coefficient R (intrachannel plasmon backscattering probability) in Eq. (47) takes the form

$$R \approx 1 - \frac{1}{\kappa^{3/2}} \frac{\lambda_a^2(4-3\lambda_a^2)}{2\sqrt{1-\lambda_a^2}}. \quad (48)$$

We see that when $\kappa \gg 1$ the difference in the Fermi velocities ceases to affect the plasmon spectrum and the spin-charge separation and the equidistant character of plasmon spectra are indeed restored. This observation could be of some interest for the problems dealing with the plasmon spectra of a multichannel ($j=1, \dots, N$) LL confined to a finite volume (with the longitudinal length L) by strong scattering barriers at $x_j=0, L$. “Hard wall” boundary conditions for the electron wave functions $\Psi_{\uparrow,\downarrow}^{(j)}(x_j=0, L)=0$ are often postulated in the

literature (see, e.g., Ref. 22). This is equivalent to electron backscattering at the boundaries without channel mixing. Although it is a rather restrictive assumption for weakly interacting electrons, it happens to be the general case for strongly interacting particles according to the above considerations (see also Ref. 25).

It is straightforward to evaluate the Josephson current using the exact plasmon spectrum for $R=1$ (i.e., when $\lambda_a=0$) and the propagators Eq. (30). The result for zero Zeeman splitting ($\Delta_Z=0$) is

$$J^{(f)}(g_c; \varphi) = J_c^{(0)} R_f(g_c) \sin \varphi, \quad (49)$$

where $J_c^{(0)} = (Dev_F/4L)(C/\pi)$ is the critical current through a 1D SNS junction and the interaction-induced renormalization factor $R_f(g_c)$ is

$$R_f(g_c) = \frac{2g_c^2}{2-g_c^2} F(2g_c^{-1}, 2g_c^{-1} - g_c; 2g_c^{-1} + 1; -1) \left(\frac{\pi a}{L} \right)^{2(g_c^{-1}-1)}. \quad (50)$$

Here $F(\alpha, \beta; \gamma; z)$ is the hyper-geometric function and g_c is the LL correlation parameter [see Eq. (22)]. For noninteracting electrons $R_f(g_c=1)=1$ and our formula has to reproduce the known expression for the Josephson current through a 1D SNS junction (see, e.g., Ref. 33). From this comparison one finds $C=\pi$.

The observation that $R \rightarrow 1$ in the limit of strong interaction ($\kappa \gg 1$) allows us to evaluate the correlation functions and the Josephson current for strongly interacting electrons with dispersion asymmetry. The Josephson current is described by Eqs. (49) and (50) after the replacement $g_c \rightarrow \kappa^{-1/2}$ and in the limit $\kappa \gg 1$. The renormalization factor now takes the form

$$R_f(\kappa \gg 1) \approx \frac{1}{\kappa} \left(\frac{\pi a}{L} \right)^{2\sqrt{\kappa}} \ll 1. \quad (51)$$

The formulas (49) and (51) show that in the considered limit the Josephson current does not depend on the parameter λ_a of dispersion asymmetry. This result is in agreement with the above physical considerations. By comparing Eq. (51) and Eq. (25) we see that the interaction suppresses the supercurrent more strongly in a long end-coupled quantum wire than in a side-coupled one.

Dispersion asymmetry affects the supercurrent of weakly interacting electrons. The influence, however, numerically is not strong even for the most favorable case of noninteracting particles. With the help of the correlation functions (41) it is easy to calculate the Josephson current of noninteracting electrons with dispersion asymmetry

$$J^{(f)}(\lambda_a, \Delta_Z; \varphi) = J_c^{(0)} R(\lambda_a) \cos \left[\frac{\Delta_Z}{2} \left(\frac{1}{\Delta_{L1}} + \frac{1}{\Delta_{L2}} \right) \right] \sin \varphi. \quad (52)$$

Here $J_c^{(0)}$ is the critical current in the absence of dispersion asymmetry [see Eq. (49)] and $R(\lambda_a)$ is the renormalization factor induced by the asymmetry of electron dispersion

$$R(\lambda_a) = \frac{\pi\lambda_a(1-\lambda_a^2)}{\sin(\pi\lambda_a)} \simeq \begin{cases} 1 + (\pi^2/6 - 1)\lambda_a^2, & \lambda_a \ll 1, \\ 2, & \lambda_a \rightarrow 1. \end{cases} \quad (53)$$

We see from Eq. (53) that the dispersion asymmetry always slightly enhances the critical current. The analysis of the Josephson current in a 1D SQWS junction in the presence of dispersion asymmetry was performed in Ref. 23 using the Andreev level approach. It was shown that the observed enhancement of the Josephson current is due to less perfect cancellations (different Fermi velocities) of the partial supercurrents carried by adjacent Andreev levels. It is interesting to notice here that the influence of spin-orbit interactions on a persistent supercurrent and on a persistent current in a 1D normal metal-ring are quite different. As we see from our analysis, the Rashba interaction either enhances the critical Josephson current or does not affect it at all depending on the geometry of the SNS junction. In contrast, spin-orbit effects are known³⁴ to suppress persistent currents in 1D normal metal rings (see also Ref. 35, and references therein).

V. THE RASHBA EFFECT, CHIRAL ELECTRONS IN 1D QUANTUM WIRES AND THE JOSEPHSON CURRENT IN S/LL/S-JUNCTION

Now we consider the limit of strong Rashba interaction. In this case the electrons in a quasi-1D quantum wire behave like truly chiral particles, so that the spin polarization of an electron irrespective of its subband index is determined by the direction of electron motion along the wire—right-moving and left-moving electrons have opposite spin projections.¹⁹ We will assume for definiteness (it depends on the sign of the Rashba coupling) that “R” electrons are “down” polarized and “L” electrons are “up” polarized (as indicated by the dashed arrows in Fig. 1). We have already seen in Sec. II, that the left/right symmetry breaking in the presence of the Zeeman interaction results in the appearance of an anomalous phase shift in the Josephson current. Physically it means that when the spin projection is correlated with the direction of motion (left, right), the magnetic field, via the Zeeman interaction, induces partial Josephson currents (for each subband “1” and “2”) even if the superconducting phase difference in the SNS junction is zero. For the spin alignments assumed in Refs. 17,18 (weak Rashba interaction) the subbands contribute to the Josephson current with opposite signs and therefore the anomalous supercurrent vanishes for symmetrical spectrum $v_{1F}=v_{2F}$. Hence the electron dispersion asymmetry is an indispensable property for getting an anomalous Josephson current in the regime of weak Rashba interactions. In the limit of strong SO interactions when all right(left)-moving particles have parallel spins, the contributions of the two subbands have the same sign and the existence of electron dispersion asymmetry ceases to be crucial for the appearance of an anomalous (at $\varphi=0$) Josephson current.

What is more important are the spin-flip processes which may take place in the transition regions between the 2D (or 3D) electron reservoirs (superconducting leads in our case) and the 1D quantum wire with a pronounced Rashba effect.

Electrons in the reservoirs have two possible spin states, while deep inside the wire, where the SO interaction is strong, the electron spins have to be aligned according to the above discussed prescription. So particles with the “wrong” spin projection should be either reflected or turn their spins toward the “right” direction. Physically, the spin flips are induced by the effective magnetic field each electron feels in its rest frame in the presence of spin-orbit interactions.

Strong spin-orbit interaction can reverse the spin projection as a result of electron backscattering. In forward scattering, spin flips can be induced by magnetic impurities at the N/S interfaces. In the absence of magnetic scattering (the case considered in this paper) the particles with “wrong” spin projection will be backscattered when entering a QW with strong Rashba interaction.

One can imagine two different types of transition (lead-wire) regions. In the case when the SO interaction is changed abruptly at the lead/wire interfaces, the spin-flips induced by the Rashba interaction will be accompanied by backscattering of electrons with both “up” and “down” spin projections. Such spin nonadiabatic contacts were studied in Ref. 19 when evaluating normal electron transport through a 1D quantum wire with strong Rashba interaction. In this model the transparency of the junction depends on the spin-orbit coupling and due to strong scattering at the wire-lead interfaces the normal electric current is partially suppressed.

Another possibility is to have adiabatic contacts where both the Rashba interaction and the electrical confinement potential are switched on smoothly over a length $\lambda_{SO} \sim \lambda_{lc}$ much larger than the Fermi wavelength λ_F . Then only particles with “wrong” spin projection will be backscattered. The accumulated magnetic moment and the charge of backscattered electrons for adiabatic contacts are distributed over a length $\lambda_{SO} (L \gg \lambda_{SO} \gg \lambda_F)$ and they can not induce backscattering of electrons with the “right” spin projection.

It is straightforward to calculate the Josephson current through an adiabatic junction. In a junction with adiabatic contacts and strong Rashba interaction right-moving spin-“down” and left-moving spin-“up” electrons are perfectly transmitted. This is exactly what one needs to form the maximum supercurrent. Electrons in the two subbands (“1” and “2”) contribute to the Josephson current with their respective Fermi velocities. At low temperatures the total critical current expressed in terms of the average Fermi velocity v_F is identical to the one in a junction without s-o interaction. So even a strong Rashba effect does not influence the Josephson current through a perfect S/QW/S junction (see also Ref. 16). This is not the case when both the Zeeman and Rashba interactions are present. Since the electron-electron interaction does not renormalize the Josephson current through a perfectly transmitting S/LL/S junction,¹⁰ we can evaluate the current using the model of noninteracting electrons with the bare spectrum shown in Fig. 1. The corresponding Andreev bound states are described by two ($j=1, 2$) independent sets of energy levels

$$E_{n_j, \eta_j}^{(j)} = \pi \Delta_L^{(j)} \left(n_j + \frac{1}{2} + \eta_j \frac{\varphi + \chi_j}{2\pi} \right), \quad (54)$$

where the integers $n_j=0, \pm 1, \pm 2, \dots$, and $\eta_j=\pm 1$ are the standard quantum numbers of the Andreev-Kulik spectrum³⁶

$\Delta_L^{(j)} = \hbar v_{jF}/L$ characterize the spacings of Andreev levels $\chi_j = \Delta_Z/\Delta_L^{(j)}$ are the magnetic phase shifts induced by the Zeeman interaction. The Josephson current for the spectrum Eq. (54) at low temperatures takes the form

$$J(\varphi, \Delta_Z) = \frac{e}{\pi L} \sum_{j=1}^2 v_{jF} \sum_{k=1}^{\infty} (-1)^{k+1} \frac{\sin k(\varphi + \chi_j)}{k}. \quad (55)$$

We see from Eq. (55) that the Zeeman interaction induces an anomalous supercurrent (at $\varphi=0$) which for large splittings $\Delta_Z \sim \Delta_L^{(j)}$ is of the order of the critical Josephson current in a perfectly transmitting SNS junction.

Now we consider the opposite limiting case, when an abrupt change (on the scale of the Fermi wavelength) both of the Rashba interaction and the electrostatic potential forms tunnel barriers for the charge and spin transport through the N/S interfaces. In our previous calculations (see Secs. II–IV) we assumed that only spin-conserving normal electron scattering occurs at the N/LL junction regions. We have to modify this calculation procedure to take into account spin flips which accompany electron backscattering at the barriers. Spin-dependent scattering induced by the Rashba interaction results, generally speaking, in a dependence of the junction transparency on the strength of the Rashba coupling $D_{\text{eff}}(\alpha_R)$. However, for poor contacts, $D \ll 1$, this effect is not significant because it cannot strongly modify the junction transparency [$D_{\text{eff}}(\alpha_R) \sim D$ by an order of magnitude]. The main new complication in comparison with the calculation scheme of Secs. II–IV is that in the general situation we have to account for two-channel normal electron backscattering at the junction interfaces. The situation is simplified when the electron-electron interaction is strong. As was shown in Sec. IV, the interchannel (“1” ↔ “2”) plasmon backscattering at the N/LL interfaces is suppressed in the limit of strong repulsive interactions. In our case it means that only intrachannel (“1” ↔ “1”, “2” ↔ “2”) electron backscattering survives for strongly interacting electrons²⁵ and we can use in this limit a simple quantization procedure for plasmons (LL with open ends²⁴) to evaluate the correlation functions. Notice that now in Eq. (12) the magnetic phases $\Delta_Z/\Delta_{1(2)}$ appear with the same sign. It results in completely different behavior of an $S/I/LL/I/S$ junction in a magnetic field for a weak and a strong Rashba effect. After straightforward calculations the desired expression for the Josephson current through a strongly interacting LL takes the form

$$J^{(R)}(\varphi) \approx J_c^{(0)} R_f \sin \left[\varphi + \frac{\Delta_Z}{2} \left(\frac{1}{\Delta_{L1}} + \frac{1}{\Delta_{L2}} \right) \right] \times \cos \left[\frac{\Delta_Z}{2} \left(\frac{1}{\Delta_{L1}} - \frac{1}{\Delta_{L2}} \right) \right], \quad (56)$$

where the interaction-induced renormalization coefficient R_f is determined by Eq. (51). As was already evident from physical considerations, the anomalous supercurrent $J^{(R)}(\varphi=0)$ in the limit of strong Rashba interaction is induced by a magnetic field ($\Delta_Z \neq 0$) even in the absence of any electron dispersion asymmetry. We see from Eq. (56) that the dependence of the supercurrent on magnetic field is absolutely dif-

ferent for chiral and normal electrons. In particular the critical current for symmetric electron spectrum ($v_{1F}=v_{2F}$) in the case of chiral electrons does not at all depend on the Zeeman splitting, while in the ordinary situation one gets a periodic dependence [see Eq. (21)].

At the end of this section we consider the influence of the strong Rashba interaction on the Josephson current in an $S/I/N/I/S$ junction for weakly interacting electrons. It is known³⁷ that when the electron-electron interaction is not strong resonant electron transport through a double barrier system may take place at certain conditions (see also Ref. 38). It results in a giant Josephson current in an $S/I/N/I/S$ symmetric junction.³³ How does the Rashba effect influence the resonant Josephson current? To answer this question we evaluate the Josephson current for noninteracting electrons through a symmetric $S/I/N/I/S$ junction with strong barriers. For simplicity we will neglect the effects of the Zeeman interaction in what follows.

The normal spin-dependent scattering of electrons at junction interfaces can be phenomenologically described by a 4×4 \hat{S} matrix. In the limit of a strong Rashba interaction each electron backscattering is accompanied by a spin flip. In addition, due to the induced electron dispersion asymmetry the backscattering in general case is a two-channel process. Since the particles with the “wrong” spin projection can not penetrate into QW with the strong Rashba interaction, the corresponding scattering problem can be effectively described by a 3×3 \hat{S} matrix. It is convenient to parametrize this matrix as follows:

$$S = e^{i\delta} \begin{pmatrix} s_{11} & s_{12} & \sqrt{\epsilon} \\ s_{12} & s_{11} & \sqrt{\epsilon} \\ \sqrt{\epsilon} & \sqrt{\epsilon} & -s_{33} \end{pmatrix}, \quad (57)$$

where

$$s_{11} = \frac{1}{2}(\tau\sqrt{1-2\epsilon} + \sqrt{\tau^2 + 2\epsilon\rho^2}), \quad (58)$$

$$s_{12} = -\frac{1}{2}(\tau\sqrt{1-2\epsilon} + \sqrt{\tau^2 + 2\epsilon\rho^2}) + e^{i\delta}\sqrt{1-2\epsilon}, \quad (59)$$

$$s_{33} = e^{-i\delta}\sqrt{1-2\epsilon}. \quad (60)$$

Here the parameter $0 \leq \epsilon \leq 1/2$ characterizes the barrier transparency ($\epsilon=0$ corresponds to the limit of the infinite barrier), τ and ρ are the intrachannel (τ) and interchannel (ρ) backscattering amplitudes $\tau^2 + \rho^2 = 1$ (for simplicity we will consider them as real quantities) and the phase $\delta = \arctan(\rho/\tau)$.

Using the standard procedure it is straightforward with the help of Eqs. (57) and (58) to calculate the spectrum of Andreev levels in an $S/I/N/I/S$ junction. Since the results for the general case are very cumbersome and lengthy, we consider the limit of a weak tunneling ($\epsilon \ll 1$) and will be interested only in the resonant electron transport. In this case the critical Josephson current through the junction is known³³ (see also Ref. 39) to be proportional to ϵ (the nonresonant

Josephson current is proportional to ϵ^2). To the first order in ϵ the spectrum of Andreev bound states in a long junction takes the form [we assume that $\epsilon \ll 1$ and $\epsilon(\rho/\tau)^2 \ll 1$]

$$E_n^\pm = E_n^0 + 2\epsilon \times \frac{\cos \beta_- - \cos \beta_\pm \pm \sqrt{(\rho/\tau)^2 \sin^2 \beta_\pm + \tau^2 \sin^2 \beta_n \cos^2(\varphi/2)}}{\tau^2 \beta'_- \sin \beta_- - \beta'_\pm \sin \beta_\pm}, \quad (61)$$

where $\beta_\pm = \beta_1 \pm \beta_2$ and $\beta_j = L\epsilon/\hbar v_{jF}$, ($j=1, 2$). In Eq. (61) $\beta'_\pm \equiv \partial\beta/\partial\epsilon$ and the energy in the dynamical phases $\beta_\pm(\epsilon)$ should be taken at $\epsilon = E_n^0$, where the energies E_n^0 are determined by the following dispersion equation [compare with Eq. (32)]:

$$\cos^2\left(\frac{\beta_\pm}{2}\right) = \tau^2 \cos^2\left(\frac{\beta_-}{2}\right). \quad (62)$$

According to Eqs. (61) and (62) the spectrum of Andreev bound states in the general case is a set of quasirandom energy levels. Notice that the resonance spectrum, Eq. (61), holds when $k_{1F}/k_{2F} = k_1/k_2$ where $k_{1,2}$ are the integers and the length L of the junction satisfies the resonance condition $(k_{1F} + k_{2F})L = \pi(k_1 + k_2)$.

Let us consider the limit $\rho \rightarrow 0$ when the Josephson current through the junction can be analytically evaluated. This case physically corresponds to the situation when backscattering at the boundaries does not mix the channels. It is realized for the ‘‘hard wall’’ boundary conditions (see the discussion in Sec. III). The partial Josephson currents at $T = 0$ ($J_{n,\pm}^{(j)} = (e/\hbar)(\partial E_n^\pm/\partial\varphi)$) in this limit are

$$J_{n,\pm}^{(j)} = \pm \epsilon \frac{e v_{jF}}{4L} \frac{\sin \varphi}{|\cos(\varphi/2)|}; \quad j = 1, 2; \quad n = 0, -1, -2, \dots \quad (63)$$

These currents exactly coincide with the resonant currents found in Ref. 33. For each quantum number $n < 0$ and given channel index j the J_\pm partial currents contribute to the total current with opposite signs and therefore cancel each other. The only surviving currents $J_{0,+}^{(j)}$ correspond to the levels $E_0^- < 0$ which have no filled partner states ($E_0^+ > 0$). Therefore at low temperatures $T \ll T_r^{(j)} = \epsilon(\hbar v_{jF}/L)$ and for the ‘‘hard-wall’’ b.c.’s the Josephson current through the symmetric junction with a strong Rashba interaction is resonant. It takes the form

$$J_r = \epsilon \frac{e v_{1F} + v_{2F}}{L} \frac{\sin \varphi}{4 |\cos(\varphi/2)|}. \quad (64)$$

Note that the analogous resonant persistent current was predicted in Ref. 40 for a normal metal-ring with a double barrier structure. It is also useful to notice that in the considered limiting case all transverse channels in a multichannel (N_\perp) quantum wire contribute coherently to the Josephson current resulting in a giant supercurrent for $N_\perp \gg 1$.

The giant Josephson current is washed out by thermal smearing even at relatively small temperatures $T \sim \max(T_r^{(j)})$. The resonance effect is also absent in the pres-

ence of a normal electron backscattering with a sufficiently strong channel mixing $\rho > \epsilon$. In this case a gap in the spectrum Eq. (61) is opened at the Fermi energy (for $\rho \sim \tau$ this gap is of the order of $\hbar v_F/L$) and the resonant Josephson current disappears even at $T \rightarrow 0$. Since there are no physical reasons for the condition $\rho \ll \epsilon \ll 1$ to be generally valid, the presence of the strong Rashba interaction should lead to a suppression of the resonance effects in the supercurrent even for symmetric junctions and weakly interacting electrons.

VI. CONCLUSION

The problem we have studied allows one to consider the interplay of proximity-induced superconductivity and the Rashba, Zeeman, and Coulomb interactions on the transport properties of quasi-1D quantum wires. We have shown that the interplay of Rashba and Zeeman effects strongly influences the supercurrent. The Rashba effect in quantum wires results in a strong correlation between electron spin polarization and the direction of electron motion.^{17,19} In other words a strong Rashba interaction creates chiral particles in the 1D electron system. The influence of a magnetic field via the Zeeman interaction on chiral particles leads to the appearance of a net electric current in the wire. When the leads that the quantum wire is attached to are superconducting, a supercurrent is induced even for zero phase difference across the junction. The effect exists already for noninteracting particles. It is strongly sensitive to any electron dispersion asymmetry and the induced Josephson current is small for weak Rashba coupling. On the contrary, in the regime of a strong Rashba interaction the anomalous phase shift in the current-phase relation can be large for large Zeeman splittings. An induced anomalous Josephson current appears even in the absence of any electron dispersion asymmetry and is of the order of the critical current.

It is well known^{10,27} that the Josephson current in a perfectly transmitting junction (i.e., without normal electron backscattering) is not influenced by the Coulomb interaction. In contrast, any potential barrier inside the normal region which induces electron backscattering is renormalized (upwards) by the repulsive interaction (the Kane-Fisher effect⁶) and therefore strongly suppresses the supercurrent through a (poorly transmitting) $S/I/LL/I/S$ junction.^{10,11,22,27} We have shown that the electron dispersion asymmetry, which is induced by the Rashba interaction in quasi-1D quantum wires,^{17,18} is significant for the superconducting properties of an LL junction only for weak or moderate Coulomb interactions. In this case the interplay of interaction and dispersion asymmetry leads to an intricate interference pattern in the plasmon quantum dynamics in a finite length two-channel LL and makes the plasmon spectrum quasirandom. Even for noninteracting electrons the electron dispersion asymmetry induced by the Rashba interaction leads to a multichannel character of electron backscattering at NS interfaces. It results in quasirandom character of Andreev bound states in a long $S/I/N/I/S$ junction. We showed that the resonance effects, which are significant for the transport properties of symmetric junctions, survive in the presence of strong Rashba interaction only for special (‘‘hard wall’’) boundary conditions at NS interfaces.

A strong Coulomb interaction suppresses this kind of quantum behavior and restores a regular (equidistant) plasmon spectrum. Notice that the tendency of strong Coulomb interactions to suppress quantum interference can be traced in different 1D electronic systems, for instance, in a LL double barrier (absence of resonant tunneling for a strong repulsive interaction³⁷) or in mesoscopic coupled rings (ordering effect of Coulomb interaction on persistent current oscillations⁴¹).

ACKNOWLEDGMENTS

This research is supported by the Royal Swedish Academy of Sciences (KVA) and by the Swedish Research Council (L.I.G., R.I.S.). The authors thank E. Bezuglyi, Yu. Galperin, L. Gorelik, and V. Shumeiko for numerous fruitful

discussions. I.V.K. and A.M.K. acknowledge the hospitality of the Department of Applied Physics at Chalmers University of Technology and Göteborg University, Sweden. A.M.K. also gratefully acknowledges the hospitality of the Theoretische Physik III Institut, Ruhr-Universität Bochum, Germany and the financial support from the ESF 'Novel Applications of Josephson Junctions in Quantum Digital Circuits (PiSHIFT)' and SFB 491. I.V.K. gratefully acknowledges discussions with B. Altshuler, L. Glazman, V. Kravtsov, and A. Nersisyan, and the hospitality and the financial support from the Abdus Salam ICTP (Trieste, Italy), where this work was completed.

APPENDIX

The canonical pseudo-orthogonal transformations, which diagonalize the Luttinger-liquid Hamiltonian (1) are²⁵

$$\begin{pmatrix} \rho_{R\uparrow} \\ \rho_{L\downarrow} \\ \rho_{R\downarrow} \\ \rho_{L\uparrow} \end{pmatrix} = \begin{pmatrix} \cosh \vartheta_1 \cos \psi & \sinh \vartheta_1 \cos \psi & -\cosh \vartheta_2 \sin \psi & -\sinh \vartheta_2 \sin \psi \\ \sinh \vartheta_1 \cos \psi & \cosh \vartheta_1 \cos \psi & -\sinh \vartheta_2 \sin \psi & -\cosh \vartheta_2 \sin \psi \\ \cosh \vartheta_3 \sin \psi & \sinh \vartheta_3 \sin \psi & \cosh \vartheta_4 \cos \psi & \sinh \vartheta_4 \cos \psi \\ \sinh \vartheta_3 \sin \psi & \cosh \vartheta_3 \sin \psi & \sinh \vartheta_4 \cos \psi & \cosh \vartheta_4 \cos \psi \end{pmatrix} \begin{pmatrix} \rho_{R1} \\ \rho_{L1} \\ \rho_{R2} \\ \rho_{L2} \end{pmatrix}, \quad (\text{A1})$$

where the "rotation angles" ϑ_j and ψ are expressed in terms of the Fermi velocities v_{1F} , v_{2F} and the interaction strength V_0 by the following equations:

$$\vartheta_1 = \frac{1}{2} \ln g_1, \quad \vartheta_2 = \frac{1}{2} \ln \left(\frac{v_{1F}}{v_{2F}} g_2 \right),$$

$$\vartheta_3 = \frac{1}{2} \ln \left(\frac{v_{2F}}{v_{1F}} g_1 \right), \quad \vartheta_4 = \frac{1}{2} \ln g_2, \quad (\text{A2})$$

$$\tan 2\psi = \frac{2V_0 \sqrt{v_{1F} v_{2F}}}{(v_{1F} - v_{2F}) [V_0 + \pi \hbar (v_{1F} + v_{2F})]}. \quad (\text{A3})$$

Here $g_j = v_{jF}/s_j$ ($j=1,2$) are the correlation parameters of a 2-channel LL and the plasmon velocities are

$$s_1 = v_{1F} \left\{ \cos^2 \psi + \left(\frac{v_{2F}}{v_{1F}} \right)^2 \sin^2 \psi + \frac{V_0}{\pi \hbar v_{1F}} \left(\cos \psi + \sqrt{\frac{v_{2F}}{v_{1F}}} \sin \psi \right)^2 \right\}^{1/2}, \quad (\text{A4})$$

$$s_2 = s_1(\psi \leftrightarrow -\psi, v_{1F} \leftrightarrow v_{2F}). \quad (\text{A5})$$

For noninteracting electrons, $V_0=0$, the correlation parameters are $g_1=g_2=1$ and, according to Eqs. (A2) and (A3) $\vartheta_1=\vartheta_4=0$, $\psi=0$. In the limit $v_{1F}=v_{2F}=v_F$ Eqs. (A2)–(A5) reproduce the well-known expressions for the correlation parameters of a spin-1/2 LL

$$\vartheta_1 = \vartheta_3 = \frac{1}{2} \ln g_c, \quad \vartheta_2 = \vartheta_4 = 0, \quad g_c = \left(1 + \frac{2V_0}{\pi \hbar v_F} \right)^{-1/2}. \quad (\text{A6})$$

¹S. Tarucha, T. Honda, and T. Saku, *Solid State Commun.* **94**, 413 (1995).

²A. Yacoby, H. L. Stormer, N. S. Wingreen, L. N. Pfeiffer, K. W. Baldwin, and K. W. West, *Phys. Rev. Lett.* **77**, 4612 (1996).

³M. Bockrath, D. H. Cobden, J. Lu, A. G. Rinzler, R. E. Smalley, L. Balents, and P. L. McEuen, *Nature (London)* **397**, 598 (1999).

⁴H. W. C. Postma, M. de Jonge, Z. Yao, and C. Dekker, *Phys. Rev.*

B **62**, R10 653 (2000).

⁵H. Ishii, H. Kataura, H. Shiozawa, H. Yoshioka, H. Otsubo, Y. Takayama, T. Miyahara, S. Suzuki, Y. Achiba, M. Nakatake, T. Narimura, M. Higashiguchi, K. Shimada, H. Namatame, and M. Taniguchi, *Nature (London)* **426**, 540 (2003).

⁶C. L. Kane and M. P. A. Fisher, *Phys. Rev. Lett.* **68**, 1220 (1992).

⁷D. L. Maslov and M. Stone, *Phys. Rev. B* **52**, R5539 (1995).

⁸V. V. Ponomarenko, *Phys. Rev. B* **52**, R8666 (1995).

- ⁹I. Safi and H. J. Schulz, Phys. Rev. B **52**, R17 040 (1995).
- ¹⁰D. L. Maslov, M. Stone, P. M. Goldbart, and D. Loss, Phys. Rev. B **53**, 1548 (1996).
- ¹¹R. Fazio, F. W. J. Hekking, and A. A. Odintsov, Phys. Rev. Lett. **74**, 1843 (1995).
- ¹²E. I. Rashba, Fiz. Tverd. Tela (Leningrad) **2**, 1224 (1960) [Sov. Phys. Solid State **2**, 1109 (1960)]; Yu. A. Bychkov and E. I. Rashba, J. Phys. C **17**, 6039 (1984).
- ¹³J. Nitta, T. Akazaki, H. Takayanagi, and T. Enoki, Phys. Rev. Lett. **78**, 1335 (1997).
- ¹⁴T. Schäpers, G. Engels, J. Lange, T. Klocke, M. Hollfelder, and H. Lüth, J. Appl. Phys. **83**, 4324 (1998).
- ¹⁵D. Grundler, Phys. Rev. Lett. **84**, 6074 (2000).
- ¹⁶E. V. Bezuglyi, A. S. Rozhavsky, I. D. Vagner, and P. Wyder, Phys. Rev. B **66**, 052508 (2002).
- ¹⁷A. V. Moroz and C. H. W. Barnes, Phys. Rev. B **60**, 14 272 (1999).
- ¹⁸A. V. Moroz, K. V. Samokhin and C. H. W. Barnes, Phys. Rev. Lett. **84**, 4164 (2000); Phys. Rev. B **62**, 16900 (2000).
- ¹⁹M. Governale and U. Zülicke, Phys. Rev. B **66**, 073311 (2002).
- ²⁰A. De Martino and R. Egger, Europhys. Lett. **56**, 570 (2001).
- ²¹A. I. Buzdin, L. N. Bulayevski, and S. V. Panyukov, Pis'ma Zh. Eksp. Teor. Fiz. **35**, 147 (1982).
- ²²J.-S. Caux, A. Lopez and D. Suppa, Nucl. Phys. B **651**, 413 (2003).
- ²³I. V. Krive, L. Y. Gorelik, R. I. Shekhter, and M. Jonson, Fiz. Nizk. Temp. **30**, 535 (2004) [Low Temp. Phys. **30**, 398 (2004)].
- ²⁴M. Fabrizio and A. O. Gogolin, Phys. Rev. B **51**, 17827 (1995).
- ²⁵I. V. Krive, S. I. Kulinich, L. Y. Gorelik, R. I. Shekhter, and M. Jonson, Phys. Rev. B **64**, 045114 (2001).
- ²⁶I. S. Gradshteyn and I. M. Ryzhik, *Tables of Integrals, Series and Products* (Academic Press, New York, 1965).
- ²⁷I. Affleck, J.-S. Caux, and A. M. Zagoskin, Phys. Rev. B **62**, 1433 (2000).
- ²⁸T. Giamarchi, *Quantum Physics in One Dimension* (Oxford University Press, Oxford, 2004).
- ²⁹A. L. Shelankov, Pis'ma Zh. Eksp. Teor. Fiz. **32**, 122 (1980) [JETP Lett. **32**, 111 (1980)].
- ³⁰G. E. Blonder, M. Tinkham and T. M. Klapwijk, Phys. Rev. B **25**, 4515 (1982).
- ³¹D. Loss, Phys. Rev. Lett. **69**, 343 (1992).
- ³²A. O. Gogolin, A. A. Nersesyan, and A. M. Tsvelik, *Bosonization and Strongly Correlated Systems* (Cambridge University Press, Cambridge, 1988).
- ³³P. Samuelsson, J. Lantz, V. S. Shumeiko, and G. Wendin, Phys. Rev. B **62**, 1319 (2000).
- ³⁴Y. Meir, Y. Gefen, and O. Entin-Wohlman, Phys. Rev. Lett. **63**, 798 (1989).
- ³⁵M. Pletyukhov and V. Gritsev, Phys. Rev. B **70**, 165316 (2004).
- ³⁶I. O. Kulik, Zh. Eksp. Teor. Fiz. **57**, 1745 (1969) [Sov. Phys. JETP **30**, 944 (1970)].
- ³⁷C. L. Kane and M. P. A. Fisher, Phys. Rev. B **46**, 15233 (1992); A. Furusaki and N. Nagaosa, *ibid.* **47**, 3827 (1993).
- ³⁸H. A. Blom, A. Kadigrobov, A. M. Zagoskin, R. I. Shekhter, and M. Jonson, Phys. Rev. B **57**, 9995 (1998).
- ³⁹I. V. Krive, S. I. Kulinich, R. I. Shekhter, and M. Jonson, Fiz. Nizk. Temp. **30**, 738 (2004).
- ⁴⁰P. Sandström and I. V. Krive, Phys. Rev. B **56**, 9255 (1997).
- ⁴¹C. M. Canali, W. Stefan, L. Y. Gorelik, R. I. Shekhter, and M. Jonson, Europhys. Lett. **40**, 67 (1997).